PAPER

Check for updates

Development of humidity-responsive self-healing zwitterionic polyurethanes for renewable shape memory applications†

Hao Wen,[a] Shaojun Chen, [ID] *[a] Zaochuan Ge,[a] Haitao Zhuo,*[b] Jinlong Ling[c] and Qiao Liu[c]

This paper reports a novel humidity-responsive self-healing material based on zwitterionic polyurethanes. The material was synthesized from *N,N*-bis(2-hydroxylethyl) isonicotinamide (BINA), hexamethylene diisocyanate (HDI) and 1,3-propanesultone (PS). The self-healing of its structure, its mechanical properties and shape memory properties were carefully investigated. Results demonstrate that self-healing zwitterionic polyurethanes contain pyridine type sulfobetaines and that strong electrostatic interactions are formed between zwitterions acting as physical crosslinkers. The aggregation of zwitterions strongly influences the phase transition behavior of polyurethane. Bulk polyurethane shows a phase-separated structure with an amorphous soft phase. The damaged zwitterionic polyurethane structure can self-heal several times in the presence of moisture without any additive or external energy. As the proportion of zwitterions increases, the self-healing efficiency increases. The self-healing efficiency results are higher when the relative humidity is increased. The self-healing mechanism is ascribed to the improved ionic mobility upon hydration and to electrostatic forces which occur during drying. Furthermore, pyridine based zwitterionic polyurethanes also show good self-healing of their shape memory properties. Self-healed polyurethanes show both a good shape fixity and recovery. This work paves the way to develop stimulus-responsive self-healing materials for renewable shape memory applications.

1. Introduction

Self-healing materials are a rapidly emerging research topic that could improve the safety and prolong the lifetime of materials.[1–3] As many biological materials, self-healing materials are able to heal structural damage.[4,5] Inspired by nature, environmental stimuli such as the pH, heat and light have been successfully used to trigger self-healing behavior.[6,7] In recent years, humidity has also been used to trigger self-healing in micro-porous polymeric multilayer films. Such humidity-triggered self-healing coatings have been even proposed for hydrophobic drug delivery applications.[8,9] Most recently, Zhu *et al.* have developed a humidity-responsive self-healing polyelectrolyte film based on hydrogen bonding and metal–ligand

coordination.[10] Self-healing materials belong to the so-called smart materials, including polymers, ceramics, concrete and metals.[1,2,11–13] The self-healing polymers are particularly attractive: chemical reaction driven self-healing polymers could be divided into those operating through reversible covalent bonding and supramolecular forces.[14,15] Self-healing polymers based on supramolecular forces are able to undergo multiple healing cycles and respond to multiple stimuli. To date, hydrogen bonding,[15] ionic interactions[16,17] and π–π stackings[18] have been widely used to design a large variety of supramolecular self-healing polymers.[2] In particular, in self-healing polymers based on inonomers, ionic species both drive the physical cross-linking and the reversible formation of the network structures. Thus, polyelectrolytes containing a large fraction of ionic groups are promising self-healing materials for many potential applications, such as actuators, sensors, drug delivery systems and other functional coatings.[19–21]

Zwitterionic polymers are special polyelectrolytes which contain both anionic and cationic groups.[22] They have been widely studied in past decades for improving blood biocompatibility and antithrombogenicity.[23–25] Recently, the self-healing functionality on zwitterionic polymer is also achieved through the combination of reversible ionic interaction and H-bonding. For example, Liu *et al.* prepared a self-healing

[a]Guangdong Research Center for Interfacial Engineering of Functional Materials, Shenzhen Key Laboratory of Special Functional Materials, College of Materials Science and Engineering, Shenzhen University, Shenzhen 518060, China. E-mail: chensj@szu.edu.cn; Fax: +86-755-26534562; Tel: +86-755-26534562

[b]Shenzhen Key Laboratory of Functional Polymer, College of Chemistry and Environmental Engineering, Shenzhen University, Shenzhen, 518060, China. E-mail: haitaozhuo@163.com

[c]Shenzhen Wenhao Sencience and Technonology Ltd., Shenzhen, China

hydrogel by copolymerizing acrylamid and a betaine-type zwitterionic monomer, 3-((2-(methacryloyloxy)ethyl)dimethylammonio) propane-1-sulfonate.[16] Bai *et al.* proposed a "zwitterionic fusion" mechanism to explain the self-healing behavior of zwitterionic polymers.[17] Kostina *et al.* reported on the self-healing properties of polycarboxybetaine based nanocomposite hydrogels with superior mechanical properties.[26] Thanks to their excellent biocompatibility and antifouling properties, self-healing zwitterionic polymer are very promising for applications in the field of smart biomedical materials. However, previous investigations on zwitterionic polymer were mostly limited to the restoration of structural or mechanical properties. It is thus urgent to investigate the restoration of functionalities for smart materials. Shape memory polymers are important smart materials which have been widely investigated in past decades.[27] In a previous work, we successfully prepared zwitterionic polyurethanes displaying shape memory properties.[28,29] Preliminary results also demonstrated that the shape memory in zwitterionic polyurethane shows interesting humidity-responsive self-healing properties.[28] Few materials combine shape memory properties and self-healing properties. The possible restoration of shape memory properties would greatly promote the development of shape memory polymers. Therefore, in this work we propose a new strategy to prepare humidity-responsive self-healing zwitterionic polyurethanes (SHZPUs) based on a pyridine-type sulfobetaine prepared with *N,N*-bis(2-hydroxylethyl) isonicotinamide (BINA) and hexamethylene diisocyanate (HDI), following by ionization with 1,3-propanesultone (PS). The self-healing of both mechanical properties and shape memory functionality were carefully investigated. Results open the way to the development of stimulus-responsive self-healing renewable shape memory materials.

2. Experimental

2.1 Materials

N,N-Bis(2-hydroxylethyl) isonicotinamide (BINA) were obtained from Jiaxing Kairui Biological Technology Co. Ltd. (Zhejiang, China). Hexamethylene diisocyanate (HDI, analytical grade), 1,3-propanesultone (PS, analytical grade), dibutyltin dilaurate (DBTD, analytical grade, catalyst for polyurethane polymerisation), and dimethylforamide (DMF, High Performance Liquid Chromatography grade, solvent) were purchased from Aladdin (Shanghai, China).

2.2 Preparation of zwitterionic polyurethanes

The synthesis routine of SHZPU compounds is presented in Scheme 1. The samples composition is summarized in Table 1. A series of SHZPU samples with different BINAPS-content were synthesized by adjusting the PS/BINA molar ratio between 0.2 and 1.0, using polyurethane polymerization followed by the ring-opening reaction method.[29] Firstly, the polyurethane polymerization was carried out in a 500 mL three-neck flask filled with nitrogen and equipped with a mechanical stirrer, a thermal meter and a condenser. The raw material of 25.00 g
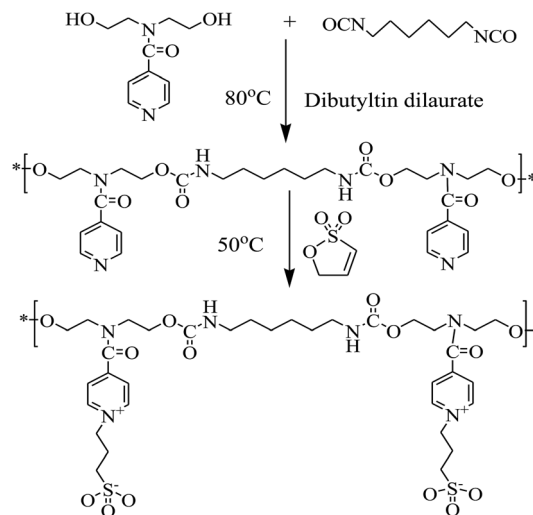
Scheme 1 Synthesis routine of pyridine based zwitterionic polyurethanes.

BINA, 22.03 g HDI, 20 mL DMF and 0.02 wt% catalyst (DBTD) were added sequentially under vigorous stirring. The reaction started immediately when the temperature was increased to 80 °C. 15 mL DMF each time were added in the reaction to control the solution viscosity. After 6 hours, the pre polymer solution was diluted to 10 wt%. Subsequently, the ring-opening reaction was performed hermetically at 50 °C for 12 hours. Finally, samples of the SHZPU were obtained by casting the 10 wt% SHZPU/DMF solution in a Teflon pan, and removing the DMF by heating at 80 °C for 24 hours in continuous air flow condition, followed by vacuum drying for 24 hours. In this study, samples were labeled as SHZPU#, in which "#" refers to the PS/BINA molar ratio.

2.3 Characterization

FT-IR spectra were measured using a Nicolet 760 FT-IR spectrometer by the FT-IR attenuated total reflection (ATR) method. 24 scans at 4 cm^{-1} resolution were signal averaged and stored as data files for further analysis.

^{1}H-NMR spectrum was recorded with Avance-400 Hz (Bruker) with D7-DMF as the solvent and tetramethylsilane (TMS) as the internal standard.

The weight percentages of C, H, N and S of the SHZPU were determined using a Vario EL III elemental analyzer (EA, Vario EL III, Germany Elementar).

The XPS analysis was made on a VG multilab2000 with Al Kα source. The anode voltage was 15 kV and the anode current was 10 mA. The core-level signals were obtained at a photoelectron take-off angle of 90°. The elemental compositions were determined on the basis of peak areas and sensitivity factor from the C_{1s}, N_{1s}, O_{1s} and S_{2p} peaks by Advantage software. All binding energy values were determined with reference to carbon, $C_{1s} = 284.6$ eV.

Differential scanning calorimetry (DSC) curves were determined using a TA Q200 instrument with nitrogen as the purge gas. Indium and zinc standards were used for calibration.

Table 1 Composition of samples and their EA results

Samples	PS/BINA molar ratio in feed	BINAPS-content in feed (wt%)	BINAPS-content by EA[a] (wt%)	Elemental composition (at%)			
				N	C	H	S
SHZPU00	0.00	0.00	0.00	14.70	55.37	6.33	0.03
SHZPU02	0.20	17.88	14.70	13.97	53.75	6.35	1.26
SHZPU04	0.40	33.43	30.18	13.54	52.21	6.37	2.45
SHZPU06	0.60	47.16	42.11	12.96	51.24	6.27	3.29
SHZPU08	0.80	59.18	57.08	12.52	49.79	6.33	4.27
SHZPU10	1.00	69.96	68.75	11.37	47.13	6.41	5.14

[a] EA: elemental analysis.

Samples were firstly heated from −60 °C to 150 °C at a heating rate of 10 °C min^{-1}, kept at 150 °C for 1 min, and then cooled to −60 °C at a cooling rate of 10 °C min^{-1}, and finally, a second heating scan was carried out from 60 °C to 200 °C.

TGA curves were recorded after drying at 100 °C by a computer-controlled TA Instrument TG Q50 system, under the following operational conditions: heating rate 10 °C min^{-1}, temperature up to 600 °C, sample weight about 5.0 mg, using the film sample in platinum crucibles, and 60 mL min^{-1} N$_2$ flow. Three or four repeated readings (temperature and weight loss) were performed using the same TG curve, each of them having at least 15 points.

Modulus testing was carried out by a computer-controlled TA Instrument DMA800 system. Specimens were cut from sample film with thickness of 0.5 mm, and the distance between two clamps was 10 mm in the initial testing status. Specimens were measured under 1.0 Hz and a heating rate of 2.0 K min^{-1}.

The morphological characterization of the dried samples were investigated by Nanonavi E-Sweep (SII Nanotechnology Inc.) atomic force microscopy (AFM) with the tapping mode and DMT mode. The samples, diluted in DMF solvent, spin-coated at 400 rpm for 10 s and then 4000 rpm for 60 s on oxidized silicon substrates. Spin-coated films were maintained in oven at 60 °C for 48 hours.

The tensile stresses of SHZPU samples were measured on an Instron 4465 texting machine at room temperature. The specimens were cut into rectangular (20 mm × 5 mm × 0.5 mm) and for tensile strength tests, and at least three samples were tested for each sample.

A stereo-optical microscope (VHX-600, Japan) was used in the study to research the healing process of various SHPUs. The specimens were scratched by glass slide with slight pressure, and to observe the course of healing by the optical microscope at 25 °C and RH 60%.

The triple-shape memory cycles produced using a one-step programming process according to the procedures described in literature.[30] The staged heating recovery conditions were investigated using a TA Instruments DMA Q800 (tension clamp, controlled force mode). Typically, the process occurs as follows: (1) the rectangular sample is heated and held at 80 °C for 10 min; (2) the sample is uniaxially elongated by a ramping force from 0.00 N to 0.175 N at a rate of 0.05 N min^{-1} and kept fully stretched at a fixed strain; (3) the sample is cooled quickly

at a rate of 30 °C min^{-1} to a low temperature at a fixed strain; (4) unloading of the extra force from 0.175 N to 0 N is performed at a rate of 0.05 N min^{-1}; (5) at the first heating stage, the sample is reheated to 80 °C at a rate of 10 °C min^{-1} and held at 80 °C for 40 min; and (5) at the second heating stage, the sample is reheated to 100 °C at a rate of 10 °C min^{-1} and held at 100 °C for another 40 min. During this process, DMA curves showing the strain, temperature and time were recorded for future analysis.

3. Results and discussion

3.1 Structure analysis

The bulk samples composition was determined with EA. The elemental species content is summarized in Table 1. The composition of BINAPS segment, corresponding to the segment of BINA grafted with PS, was deduced from the S content. The difference between the measured BINAPS segment composition and that in feed, was ascribed to the incomplete ring-opening reactions or the decomposition of BINAPS during the storing or drying. The incorporation of sulfobetaine increases with the increase of PS/BINA ratio. This clearly shows that the zwitterion was successfully grafted onto the N of pyridine rings. The molecular structure of polyurethane pre polymer (SHZPU00) and pyridine based zwitterionic polyurethanes (SHZPU04, SHZPU08) was investigated systematically with ATR-FTIR, ^{1}H-NMR and XPS. As shown in the FT-IR spectra (Fig. 1), the N–H stretching vibration was observed at approximately 3318 cm^{-1} and the characteristic carbonyl peaks were found at 1688 cm^{-1}, indicating the formation of urethane groups.[29,30] In the samples SHZPU04 and SHZPU08, the presence of SO$_3^-$ was proved by the peak at 1038 cm^{-1}. The SO$_3^-$ peak intensity in sample SHZPU08 was stronger than in sample SHPU04. The weak absorption peak from quaternary N-groups was detected at 960 cm^{-1} in samples SHZPU04 and SHZPU08. Additionally, ^{1}H-NMR spectra confirmed that the sulfobetaine segment in both SHZPU04 and SHZPU08 shows chemical shifts at 2.25, 4.75 and 8.08 ppm (Fig. 1B). Bands at 2.25 and 8.08 ppm were assigned to methylene groups (–CH$_2$–) near the pyridine ring and SO$_3^-$ groups, respectively. This confirmed that the sulfobetaine groups were grafted on zwitterionic polyurethanes. XPS spectra were acquired to characterize the N and S oxidation state (Fig. 1C). Two components are seen in S$_{2S}$ and S$_{2P}$ peaks in SHZPU04 and SHZPU08 samples, however only one is seen in the precursor
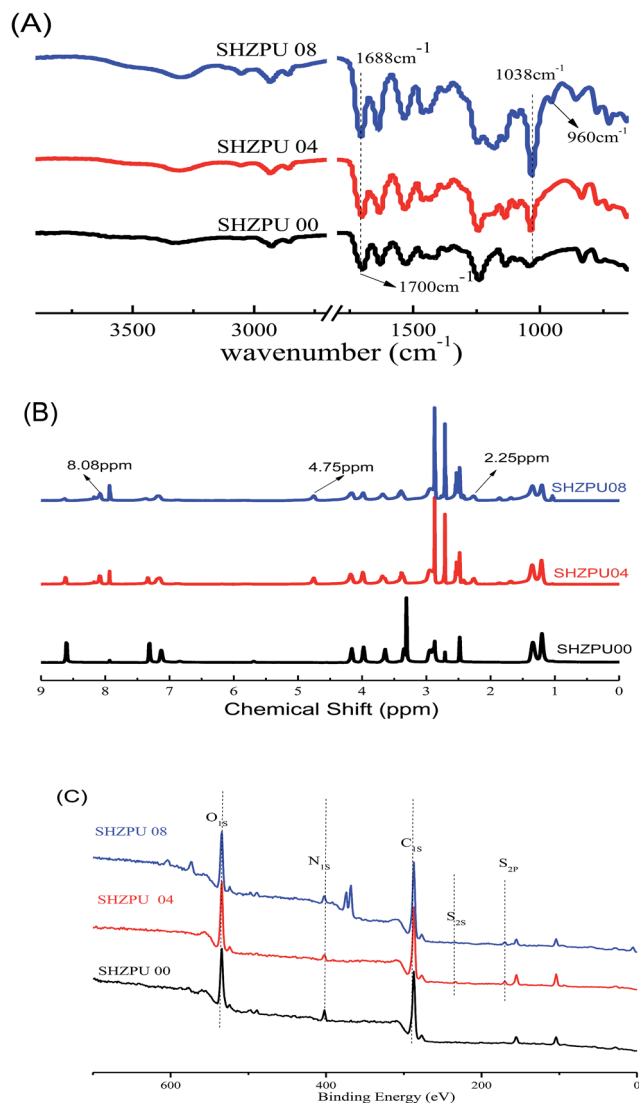
Fig. 1 Structure analysis of pyridine based zwitterionic polymers (A) FT-IR spectra; (B) ^{1}H-NMR spectra; (C) XPS survey spectra.

Fig. 2 Thermal-properties of pyridine based zwitterionic polyurethanes ((A) DSC second heating curves; (B) TGA curves).

SHZPU00; the shoulder peak was assigned to atoms from sulfobetaine (Fig. S1(a)†). Furthermore, in samples SHZPU04 and SHZPU08 two componets are clearly distinguished in the N_{1s} spectrum, the one at 402 eV binding energy corresponds to N in sulfobetaine's ternary ammonium ($>N^+$–CH_3), and the one at 400 eV to nitrogen in urethane (–N–COO) or unmodified $>N$–CH_3 groups which are also present the SHZPU00 sample (Fig. S1(b)†). XPS analysis thus confirms the formation of that the pyridine based zwitterionic polyurethanes.

3.2 Thermal properties

DSC and TGA analyses have been widely applied for studying phase transitions and thermal-stability. Fig. 2 shows that polyurethane pre-polymers and zwitterionic polyurethanes both form only one amorphous soft phase below 150 °C. The glass transition temperature (T_g) increases linearly from 23.5 °C to 57.0 °C, as the BINAPS-content is increased. This result is consistent with
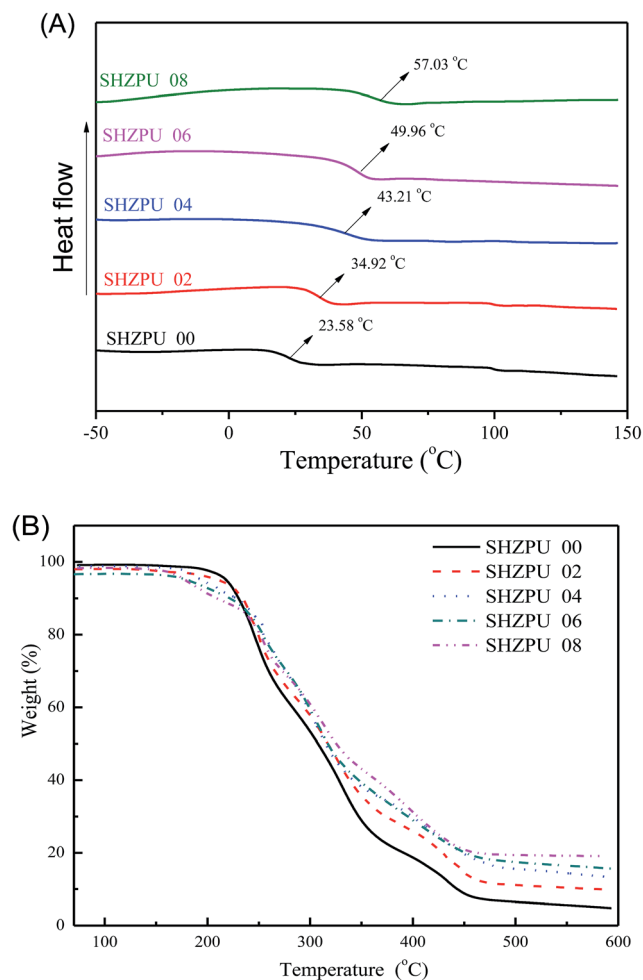
previous investigations on zwitterionic polyurethanes and relies on the fact that the aggregation of BINAPS segments and the strong electrostatic interactions strongly influence the mobility of polyurethane chains acting thus as physical crosslinking.[29] Additionally, TGA curves demonstrate that the initial decomposition occurs below 200 °C in all zwitterionic polyurethanes, indicating their limited thermal stability. Compared with the polyurethane pre-polymer (ZSMPU00), the initial decomposition temperature (T_i) shifts toward lower temperatures as the BINAPS content increases. This decomposition was also associated with the dynamics of BINAPS segments, however, this result differs from previous results on pyridine based zwitterionic polyurethanes containing MDI-BDO hard segments.[31] The possible reason is that is that the physical net point is too weak, so that the grafted zwitterions can be damaged more easily in this BINA-HDI-PS system. Finally, it is found that samples residues increases from 6.5% to 20% as the BINAPS content is increased. These residues were associated with PS units due to the presence of sulfur. These findings provide an additional powerful proof that the pyridine type sulfobetaines have been introduced into polyurethanes and that they influence the mobility and the decomposition of zwitterionic polyurethane chains.

3.3 Dynamic mechanical properties

The effects of zwitterions on the dynamical, morphological and mechanical properties of the polyurethanes were investigated with DMA (Fig. 3). Storage modulus curves demonstrate that zwitterionic polyurethanes possess a glassy modulus at low temperature range. When polyurethanes are grafted with higher BINAPS content, the glassy modulus increases. This confirms that the incorporation of zwitterions reinforce the polyurethanes structure. However, the formation of BINAPS segments might prevent the aggregation of hard segments, as suggested by the rubber modulus decreases with the increasing of the BINAPS content. It was previously reported that strong hydrogen bonding are formed between pyridine rings and urethane groups.[31] The grafting of zwitterions would replace the original hydrogen bonding of pyridine rings, influencing the aggregation of hard segments or physical net points. Additionally, both the modulus curves and tan δ curves confirm that the T_g shifts to higher temperature as the BINAPS content increases. This result is consistent with DSC results. The broad

peak in Fig. 3B also suggests the presence of a multiple phase transition among the zwitterionic polyurethane, implying a triple-shape memory effects.[32] The two overlapped peaks in Fig. 3B indicate the presence of a micro-scaled phase separation structure with a phase mixing occurring since the T_g of the soft phase shifts to higher temperature and the T_g of hard phase shifts toward lower temperatures the BINAPS content increases. AFM phase imaging was also used to study the morphology of polymers.[33] DMT modulus maps are a very good complement to phase images, in these representation, the color variation indicates differences in the value of the Young's modulus.[34] We acquired 3D-height images, 3D-phase images and 3D-DMT modulus images (Fig. 4). The multiple protrusions observed in 3D-DMT modulus images result from the high modulus of aggregated zwitterions acting as the hard phase. Hence, this analysis confirms that the morphology of zwitterionic polyurethanes mainly consist of staggered hard and soft segments.

3.4 Self-healing in structure

Self-healing properties were widely studied in past years.[2] The self-healing efficiency was mainly characterized from the restoration of the structure and the original properties.[15] Fig. 6 shows the self-healing test in sample SHZPU08. As shown in Fig. 5(A), the rectangular specimen (Fig. 5 and S1†) was cut into two parts (Fig. 5 and S2†). The two parts were then put in contact without any additives or external energy (Fig. 5 and S3†) and put in a moisture environment (*e.g.* 60% RH) at room temperature. The two parts self-healed spontaneously (Fig. 5 and S4†). The self-healing process was observed with an optical microscope (Fig. 5(B)). The sample was scratched firstly by a glass slide with a slight pressure and put at 25 °C and RH 60% conditions during which the scratch was recovered gradually (see Fig. 5a–d). Scratches disappear without any scar (Fig. 5e). Additionally, the self-healing speed was quite different in the zwitterionic polyurethanes with different BINAPS content. The SHZPU08 sample undergoes its self-healing within 100 min, while SHZPU06 and SHZPU04 samples employed 140 and 200 min, respectively. The SHZPU02 sample resulted in a incomplete self-healing after 400 min. Therefore, the self-healing speed clearly increases with the BINAPS content. This result implies that the self-healing properties are associated with electrostatic forces among zwitterions.

3.5 Self-healing in mechanical properties

Mechanical properties are a critical parameter which should be primarily restored in the self-healing materials.[35] In this experiment, the sample named A was cut in half and subsequently connected with the original section for self-repairing for 24 hours at 60% RH and 25 °C. Then sample B was obtained by repeating the test on sample A. Before testing, all samples were oven dried fully at 60 °C. In order to investigate the repeated self-healing, the strain–stress curves were acquired on both samples. Fig. 6 presents the repeated self-healing test on mechanical properties for zwitterionic polyurethanes with different BINAPS contents. The self-healing efficiency *versus*
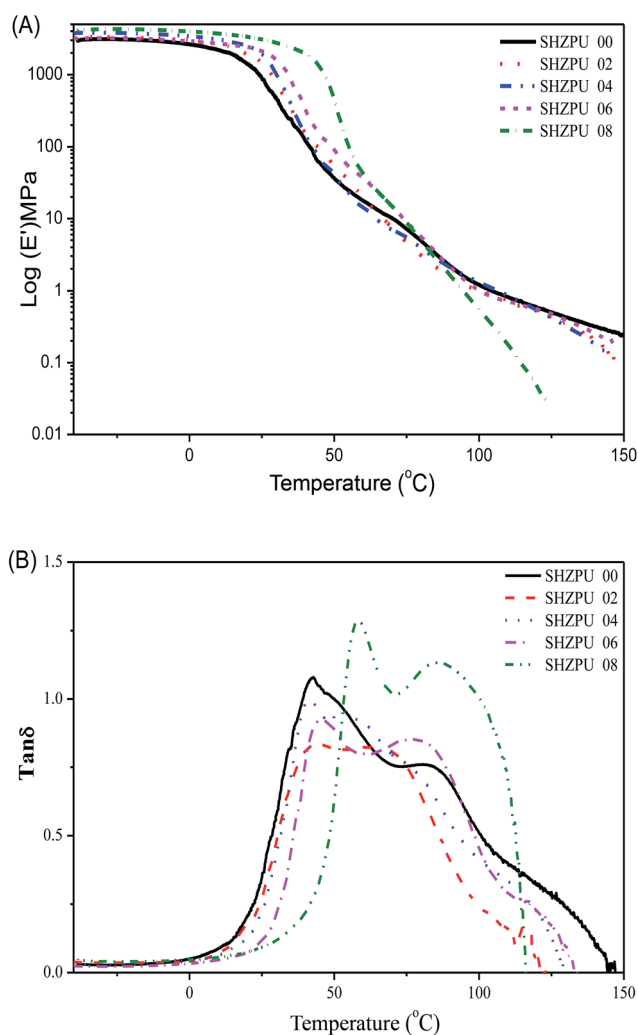

Fig. 3 DMA curves of pyridine based zwitterionic polymers ((A) storage modulus; (B) tan δ).
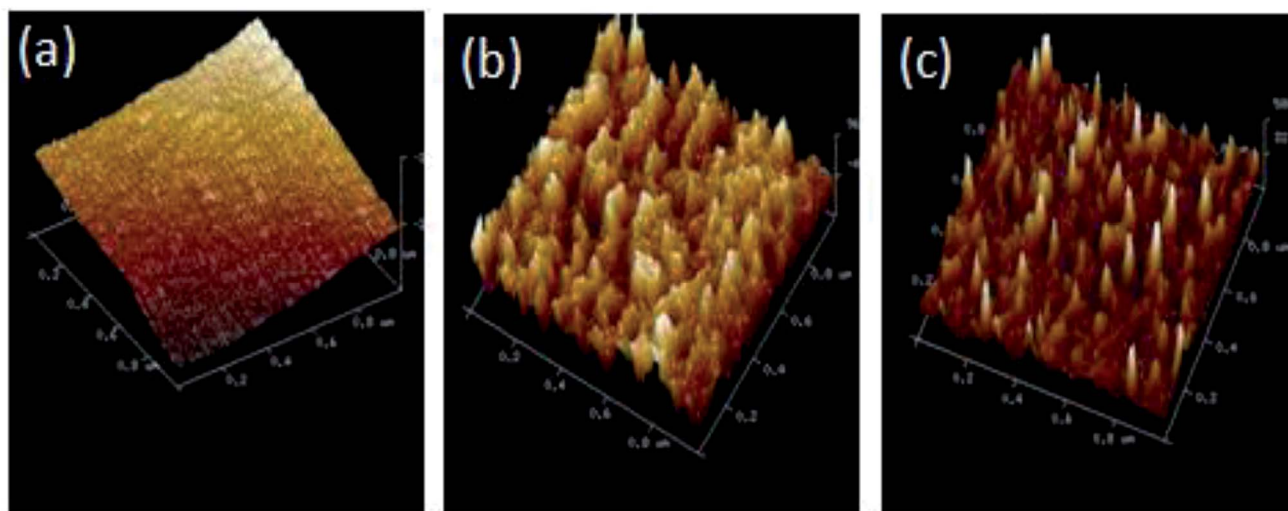
Fig. 4 AFM images ((a) height image; (b) phase image; (c) DMT moduli image) of SHZPU08.
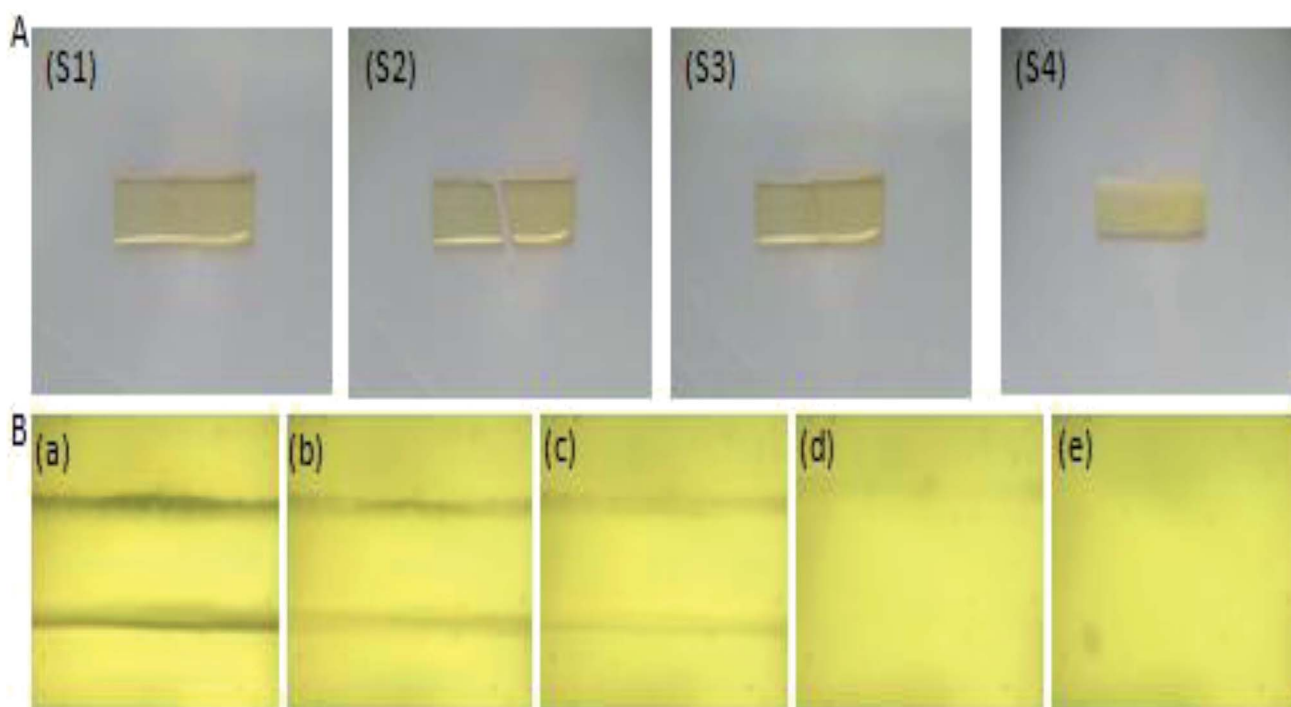

Fig. 5 Photos showing the self-healing in structure (A) and the humidity-responsive self-healing process (B) for sample SHZPU08. [S1-the original sample; S2-the cut sample; S3-the adhered sample; S4-the healed sample; a-scratched sample at 0 min; b-scratched sample at 20 min; c-scratched sample at 40 min; d-scratched sample at 60 min; d-scratched sample at 80 min; e-scratched sample at 100 min].

strain and stress are reported in Fig. S2.† In SHZPU04 and SHZPU06 samples, after the first healing strain and stress resistance are lower respect to the pristine sample which has not been damaged, moreover, healing efficiency is lower after the second healing. In sample SHZPU08, the self-healing efficiency remains high over the two healing cycles. This suggests that zwitterionic polyurethanes with higher BINAPS content have better repeated self-healing efficiency. When the PS/BINA molar ratio is higher than 0.8, zwitterionic polyurethanes

showed a self-healing efficiency higher than 101% *versus* the strain parameter, and higher than 97% *versus* the stress parameter.

The moisture content is a key factor ruling the self-healing efficiency in the zwitterionic polyurethanes. Fig. 7 presents the self-healing of mechanical properties under different RH conditions. Sample SHZPU06 was selected for this analysis. After the cut, the sample was placed in different relative humidity condition (30, 60 and 90% RH) at room temperature
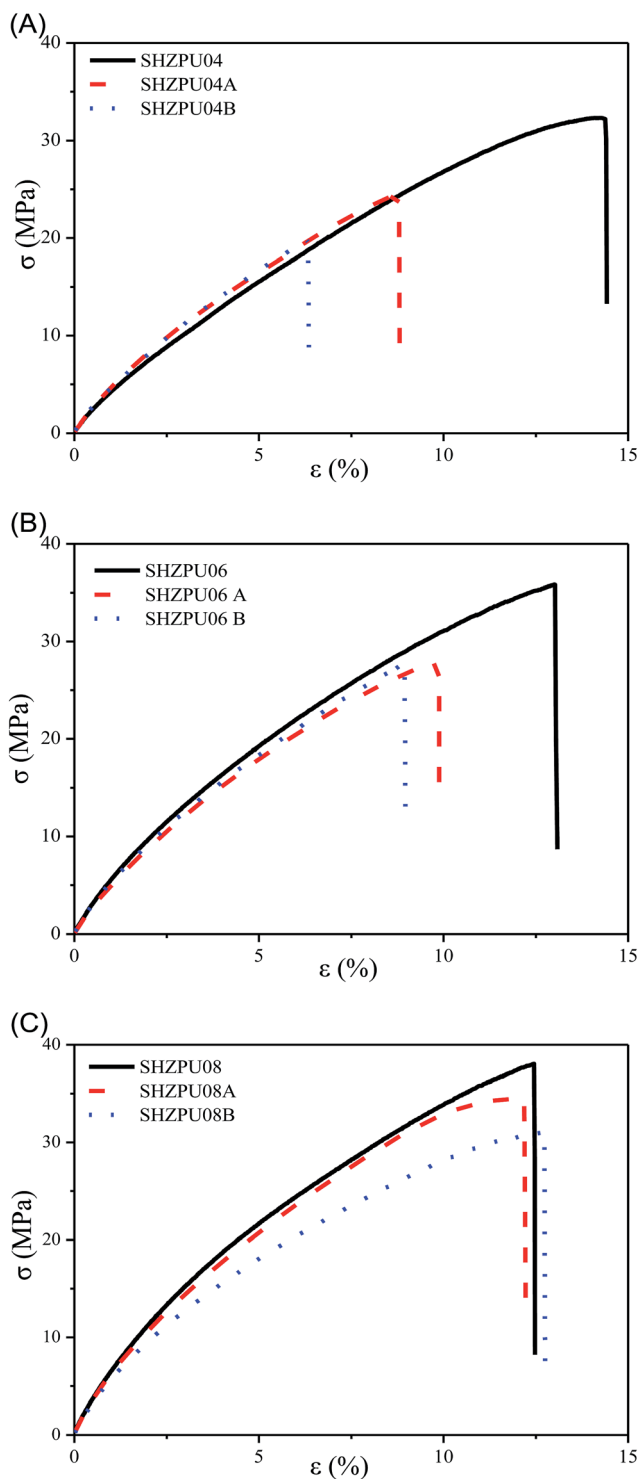
Fig. 6 Self-healing in mechanical properties for zwitterionic polyurethanes with different BINAPS content ((A) ZSHPU04; (B) ZSHPU06; (C) ZSHPU08).
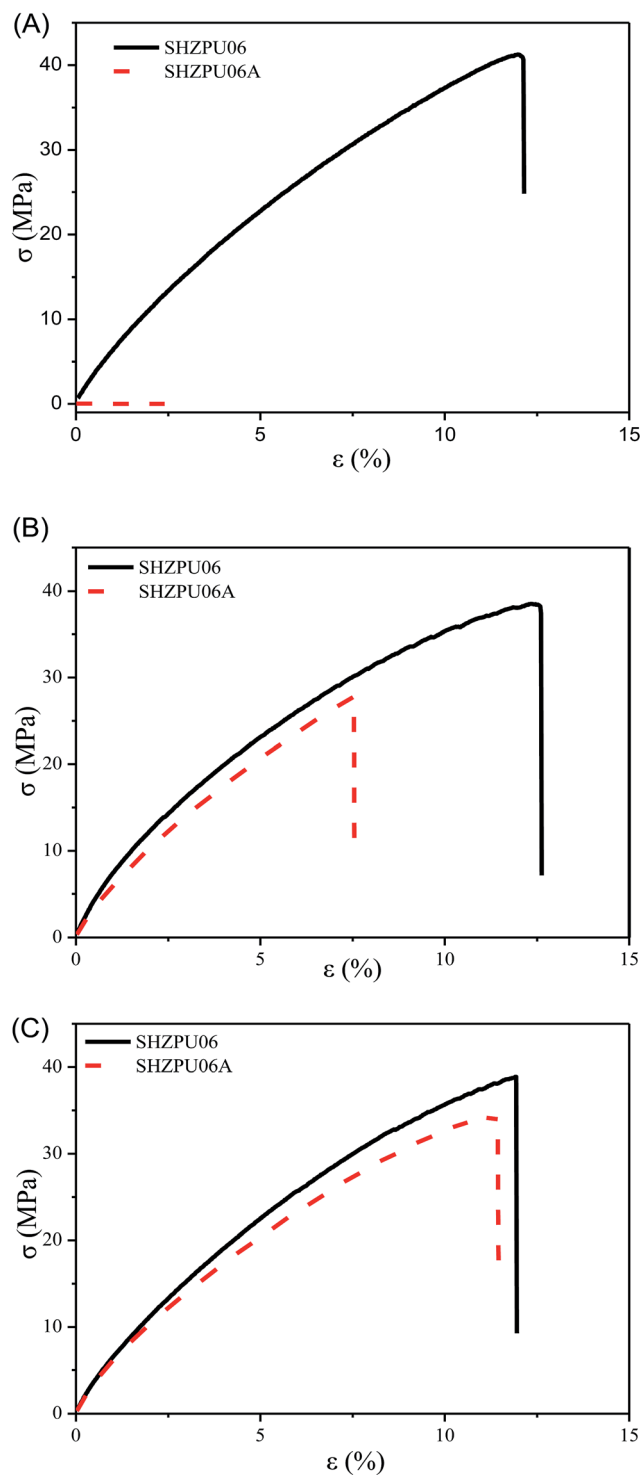

Fig. 7 Self-healing in mechanical properties for zwitterionic polyurethanes under different moisture conditions ((A) 30% RH; (B) 60% RH; (C) 90% RH).

for self-healing. Under 30% RH, the sample could difficultly self-repair. As the RH attains 60% and 90%, the self-healing efficiency *versus* the stress increases up to 72–89%, respectively, and the efficiency *versus* the strain increased up to 60% and 95% (Fig. S3†). The reason why a higher RH promotes the healing efficiency, is that a higher moisture absorption

promotes the zwitterions fusion as shown in the previous sections.

According to our findings, the self-healing mechanism of the pyridine based zwitterionic polyurethanes might be explained as follows: a strong electrostatic interaction occurs
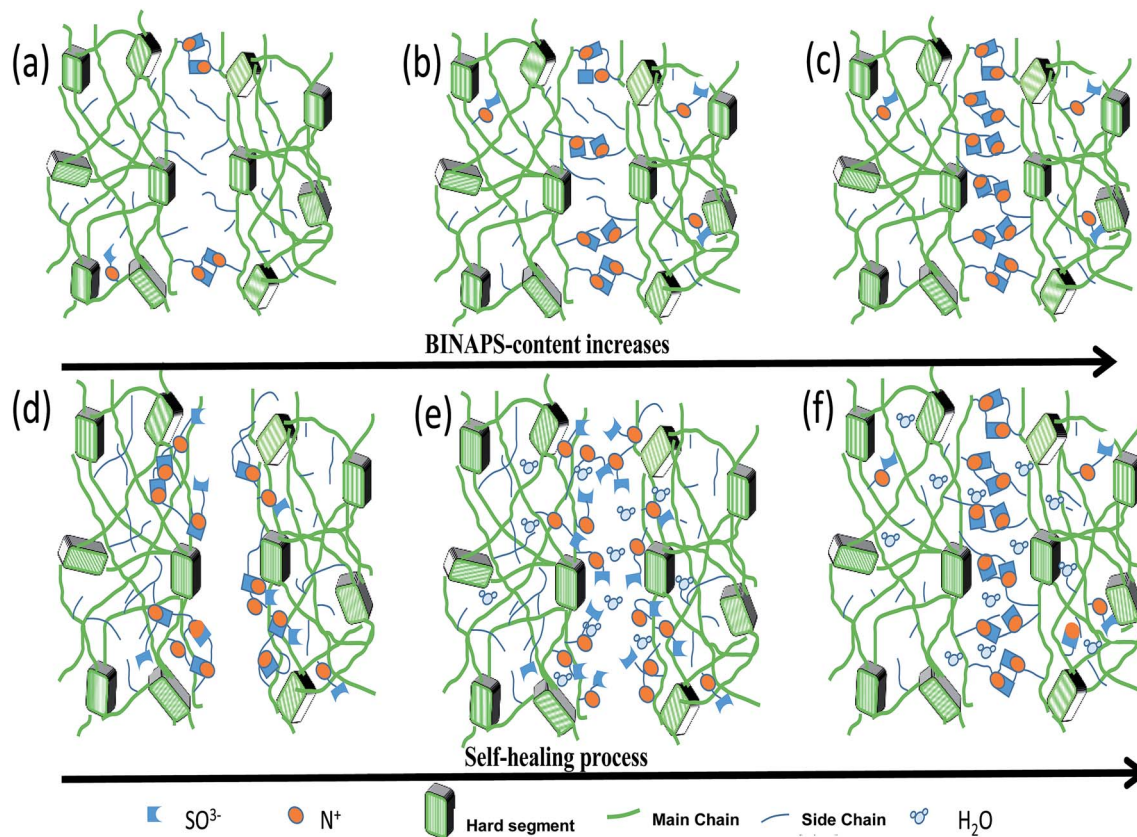
Fig. 8 Illustration for self-healing mechanism of zwitterionic polyurethanes.

between N^+ and SO_3^- ions among zwitterionic moieties. When the BINAPS content is low (SHZPU02), a small fraction of ionic bonds are formed (Fig. 8a), as the BINAPS content increases, the fraction of ionic bonds increases (Fig. 8b). Zwitterionic polyurethanes with high BINAPS content (SHZPU08) possess a large fraction of ionic bonds (Fig. 8c). The aggregation of BINAPS segments might reinforce the hard segment, acting as a physical crosslinker in zwitterionic polyurethane. In self-healing, most of the ionic bonds in zwitterionic polyurethanes are in the bulk film (Fig. 8d). The cut breaks electrostatic forces at the interface, between N^+ and SO_3^- groups; these species might move to the surface under high moisture condition due to the hydration of zwitterionic segments (Fig. 8e). Therefore, during drying, strong electrostatic forces are reformed while there are still a large fraction of ionic bonds available in the self-healed zwitterionic polyurethane (Fig. 8f). This explains why with the higher BINAPS content was associated with a higher self-healing efficiency under high RH conditions.

3.6 Self-healing in shape memory properties

Since structural and mechanical properties are self-healed perfectly in the zwitterionic polyurethane with high BINAPS content (as in sample SHZPU08), it is presumable that shape memory functionality can be also restored in this sample. In our previous investigation,[29] we reported that the zwitterionic

polyurethanes developed form the BINA monomer showed good thermal-induced multi-shape memory effects. We had also studied the triple-shape memory effect of supramolecular polyurethane complexes based on BINA monomer using a one-step programming process.[30] Sample SHZPU08 was selected for this analysis. According to the one-step programming process, the original sample SHZPU08 was firstly elongated to more than 100% strain at 60 °C. The deformation corresponding to 100% strain was fixed at 0 °C. Upon heating, the strain is recovered step by step and more than 54.5% of the strain was recovered at 60 °C. An additional 35% strain was recovered at 80 °C. The total strain recover was higher than 88% (Fig. 9(A)). Similarly, after the cut the sample was healed under moisture condition of 60% RH and 25 °C. The first healed sample was tested in the same way. Fig. 8(B) demonstrates that the healed sample exactly showed the same shape recovery process. The shape fixity yield was close to 100%, the shape recovery yield at 60 °C was 54.6% and at 80 °C was 88.2%. The reason is that apart from the cut region samples display the same phase separated microstructure in both healed sample and pristine samples. The high self-healing promoted by zwitterions fusion ensures the same performance after healing. Therefore, the shape recovery functionality can be self-healed perfectly under moisture condition without any additives.
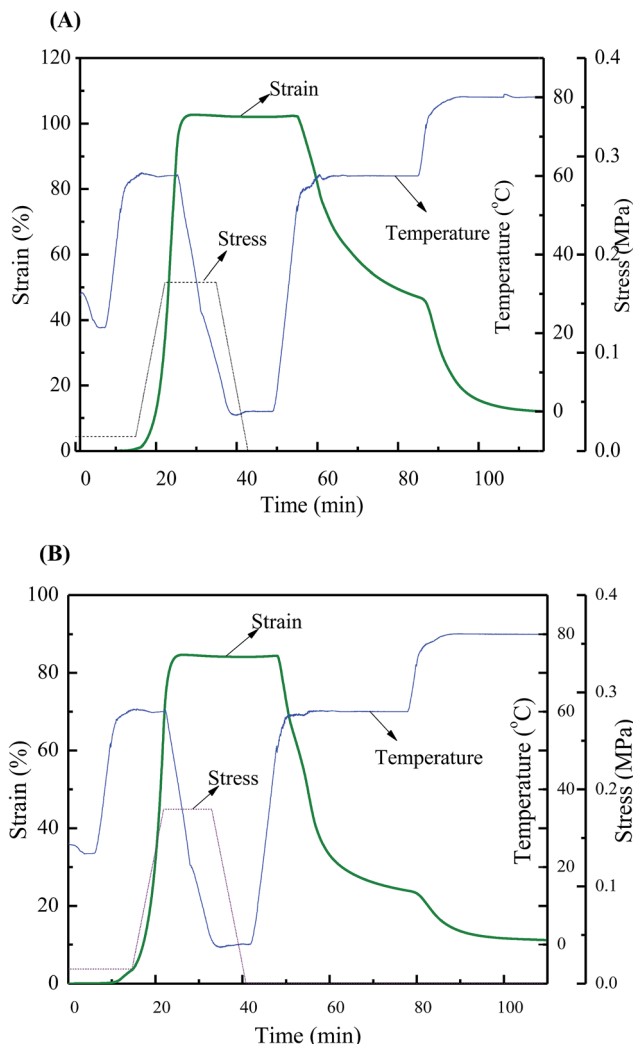
(A)

(B)

Fig. 9 The self-healing in shape memory functionality for sample SHZPU08 ((A) the original sample; (B) the first self-healed sample).

4. Conclusions

In this paper, a novel humidity-responsive self-healing zwitterionic polyurethane was synthesized from BINA, HDI and 1,3-PS. The structure, morphology, thermal-properties and self-healing properties were investigated carefully. Results show that the self-healing zwitterionic polyurethanes contain pyridine-type sulfobetaines, forming strong electrostatic interactions between zwitterions. The bulk polyurethane displays a phase-separated structure with an amorphous soft phase. We demonstrated that the pyridine based zwitterionic polyurethane have attractive self-healing properties. Above 60% RH moisture condition at 25 °C, damages can be restored without any additive or external energy. Moreover, samples showed good repeated self-healing properties allowing to restore their original mechanical properties. As the zwitterions content increases, the self-healing efficiency *versus* strain and stress increases. Finally, the self-healing efficiency is higher than 101% *versus* the strain, and higher than 97% *versus* the stress.

The healed sample also shows good triple-shape memory effect with shape fixity yield of 100% and the total shape recovery yield of 88.2%. At a high relative humidity, the self-healing improves, *e.g.* the efficiency *versus* the stress and strain are 89% and 95% at 90 RH%, respectively. The self-healing mechanism was ascribed to the motion of ionic species upon hydration and to the presence of electrostatic forces which could be reformed after the drying. Furthermore, the pyridine based zwitterionic polyurethanes also showed a good recover of their shape memory properties including shape fixing and shape recovery.

References

1 D. Y. Wu, S. Meure and D. Solomon, *Prog. Polym. Sci.*, 2008, **33**, 479–522.
2 Y. Yang and M. W. Urban, *Chem. Soc. Rev.*, 2013, **42**, 7446–7467.
3 R. X. Chang, Y. F. Huang, G. R. Shan, Y. Z. Bao, X. Y. Yun, T. L. Dong and P. J. Pan, *Polym. Chem.*, 2015, **6**, 5899–5910.
4 R. P. Wool, *Soft Matter*, 2008, **4**, 400–418.
5 K. S. Toohey, N. R. Sottos, J. A. Lewis, J. S. Moore and S. R. White, *Nat. Mater.*, 2007, **6**, 581–585.
6 P. Cordier, F. Tournilhac, C. Soulie-Ziakovic and L. Leibler, *Nature*, 2008, **451**, 977–980.
7 Y. Amamoto, H. Otsuka, A. Takahara and K. Matyjaszewski, *Adv. Mater.*, 2012, **24**, 3975–3980.
8 X. C. Chen, K. F. Ren, J. H. Zhang, D. D. Li, E. Zhao, Z. J. Zhao, Z. K. Xu and J. Ji, *Adv. Funct. Mater.*, 2015, **25**, 7470–7477.
9 Y. B. Dou, A. Zhou, T. Pan, J. B. Han, M. Wei, D. G. Evans and X. Duan, *Chem. Commun.*, 2014, **50**, 7136–7138.
10 Y. X. Zhu, H. Y. Xuan, J. Y. Ren, X. F. Liu, B. Zhao, J. H. Zhang and L. Q. Ge, *RSC Adv.*, 2016, **6**, 89757–89763.
11 B. Zhang, Z. A. Digby, J. A. Flum, E. M. Foster, J. L. Sparks and D. Konkolewicz, *Polym. Chem.*, 2015, **6**, 7368–7372.
12 J. A. Neal, D. Mozhdehi and Z. B. Guan, *J. Am. Chem. Soc.*, 2015, **137**, 4846–4850.
13 Y. L. Chen and Z. B. Guan, *Chem. Commun.*, 2014, **50**, 10868–10870.
14 K. Imato, M. Nishihara, T. Kanehara, Y. Amamoto, A. Takahara and H. Otsuka, *Angew. Chem., Int. Ed.*, 2012, **51**, 1138–1142.

15 F. Herbst, D. Dohler, P. Michael and W. H. Binder, *Macromol. Rapid Commun.*, 2013, **34**, 203–220.

16 H. Liu, C. Xiong, Z. Tao, Y. Fan, X. Tang and H. Yang, *RSC Adv.*, 2015, **5**, 33083–33088.

17 T. Bai, S. J. Liu, F. Sun, A. Sinclair, L. Zhang, Q. Shao and S. Y. Jiang, *Biomaterials*, 2014, **35**, 3926–3933.

18 S. Burattini, B. W. Greenland, D. H. Merino, W. G. Weng, J. Seppala, H. M. Colquhoun, W. Hayes, M. E. Mackay, I. W. Hamley and S. J. Rowan, *J. Am. Chem. Soc.*, 2010, **132**, 12051–12058.

19 Y. Ren, R. Y. Lou, X. C. Liu, M. Gao, H. Z. Zheng, T. Yang, H. G. Xie, W. T. Yu and X. J. Ma, *Chem. Commun.*, 2016, **52**, 6273–6276.

20 F. Luo, T. L. Sun, T. Nakajima, T. Kurokawa, Y. Zhao, K. Sato, A. Bin Ihsan, X. F. Li, H. L. Guo and J. P. Gong, *Adv. Mater.*, 2015, **27**, 2722–2725.

21 Y. Huang, P. G. Lawrence and Y. Lapitsky, *Langmuir*, 2014, **30**, 7771–7777.

22 A. B. Lowe and C. L. McCormick, *Chem. Rev.*, 2002, **102**, 4177–4189.

23 G. Li, G. Cheng, H. Xue, S. Chen, F. Zhang and S. Jiang, *Biomaterials*, 2008, **29**, 4592–4597.

24 A. Laschewsky, *Polymers*, 2014, **6**, 1544–1601.

25 C. Wang, C. Ma, C. Mu and W. Lin, *Langmuir*, 2014, **30**, 12860–12867.

26 N. Y. Kostina, S. Sharifi, A. D. Pereira, J. Michalek, D. W. Grijpma and C. Rodriguez-Emmenegger, *J. Mater. Chem. B*, 2013, **1**, 5644–5650.

27 J. Hu and S. Chen, *J. Mater. Chem.*, 2010, **20**, 3346–3355.

28 S. J. Chen, F. N. Mo, Y. Yang, F. J. Stadler, S. G. Chen, H. P. Yang and Z. C. Ge, *J. Mater. Chem. A*, 2015, **3**, 2924–2933.

29 S. J. Chen, Z. K. Mei, H. H. Ren, H. T. Zhuo, J. H. Liu and Z. C. Ge, *Polym. Chem.*, 2016, **7**, 5773–5782.

30 S. J. Chen, H. M. Yuan, S. G. Chen, H. P. Yang, Z. C. Ge, H. T. Zhuo and J. H. Liu, *J. Mater. Chem. A*, 2014, **2**, 10169–10181.

31 S. J. Chen, J. L. Hu, S. G. Chen and C. L. Zhang, *Smart Mater. Struct.*, 2011, **20**, 065003.

32 T. Xie, *Nature*, 2010, **464**, 267–270.

33 P. Schon, K. Bagdi, K. Molnar, P. Markus, B. Pukanszky and G. J. Vancso, *Eur. Polym. J.*, 2011, **47**, 692–698.

34 D. Reifer, R. Windeit, R. J. Kumpf, A. Karbach and H. Fuchs, *Thin Solid Films*, 1995, **264**, 148–152.

35 M. Q. Zhang and M. Z. Rong, *Acta Polym. Sin.*, 2012, 1183–1199.